Modeling and Simulation of Long Boom Manipulator based on Geometrically Exact Beam Theory

Lingchong Gao[1], Yingpeng Zhuo[2], Michael Kleeberger[1], Haijun Peng[2] and Johannes Fottner[1]

[1]*Chair of Materials Handling, Material Flow, Logistics, Technical University of Munich, Garching, Germany*
[2]*Department of Engineering Machenics, Dalian University of Technology, Dalian, P.R. China*

Keywords: Long Boom Manipulator, Geometrically Exact Beam, Multi-body Dynamic, Nonlinear System.

Abstract: The boom system of the aerial platform vehicle and the fire-rescue turntable ladder can be considered as a long boom manipulator. Due to the slenderness of the boom structure, there are always some vibrations occurring during the operation. In order to control the vibration, reliable dynamic modeling and simulation are necessary. In this paper, we propose a model of the long boom manipulator, especially the folding boom system, as a flexible-rigid coupled multi-body system. And the flexible long boom structure is formulated as a geometrically exact Euler-Bernoulli beam with hybrid interpolation for discretization. The governing equations of the system dynamics are established according to the principle of virtual power. A dynamic simulation of the spatial motion of the long boom manipulator is performed and the results are analyzed.

1 INTRODUCTION

Aerial platform vehicle and fire rescue turntable ladder are usually equipped with long boom systems to help personal to reach a high position. In order to make the boom as long as possible without compromising the mobility of the carriage vehicle, the boom is designed as a telescopic boom or folded boom. The boom system can be fully unfolded for operation in the meanwhile be folded for transitions on the road network. The boom system is normally equipped with a hydraulic system to provide power for actions and can be considered as a hydraulic manipulator with a long boom structure. The long boom manipulator is designed with a long and slender boom structure so that the weight can be controlled to fit the limit of bearing capacity of the vehicle axle. However it leads to another problem, the vibration occurs during the operation due to the flexibility of the boom structure. Such vibration can be stimulated by the change of the motion status, such as sudden acceleration or declaration, or the change of the external forces. Therefore the topics of dynamic simulation and vibration control of this kind of long boom manipulator have attracted some researchers to investigate.

In the work of Zuyev (Zuyev, 2005), the boom structure of the fire-rescue turntable ladder was modeled as a flexible multi-body system with the passive joint for the stabilization of the boom system, and

the hydraulic component was included in the mathematical model of the system (Sawodny et al., 2002). Pertsch applied the assumption of the Euler-Bernoulli beam theory on the description of the dynamic behavior of the fire-rescue turntable ladder as a distributed parameter model (Pertsch et al., 2009). The model has been further developed for the coupled bending-torsional vibration that occurs in the slewing motion, and the corresponding active control for the vibration damping was also developed and tested in real operation (Pertsch and Sawodny, 2016). Nguyen developed a multi-body dynamic model with a chain of rigid bodies connected to each other end by end with rotational spring and dampers to reflect the flexibility of the ladder. He also included a model of rope in the system to investigate the effect of the pre-tensioned rope to the vibration of the ladder structure during the luffing operation (Nguyen et al., 2019). In our recent work (Gao et al., 2019), we investigated the dynamic response of the long boom manipulator with the consideration of the hydraulic drive system. The mathematical models of the hydraulic system and boom structure, which was modeled as a planar Timoshenko beam, were established as port-Hamiltonian formulation and a co-simulation of this structure-hydraulic system is performed in the environment of Simulink.

An accurate dynamic model of the long boom manipulator is the prerequisite for the control design to suspension the vibration. Based on our previous

work, we would like to investigate the spatial dynamic performance of the long boom manipulator. Then we need a suitable description for the dynamical behavior of the flexible boom in space. The deformation of the boom is considerably small compared with the length of the boom and the rotation and the displacement of the rigid body are rather large. This flexible-rigid coupled problem of geometrical non-linearity involving small flexible deformation draws our attention to the achievement of the development of geometrically exact beam element formulation.

The geometrically exact beam theory was proposed and developed by Reissner (Reissner, 1973) (Reissner, 1972) and Som (Simo, 1985) (Simo and Vu-Quoc, 1986) (Simo, 1988) model the geometrically nonlinear beams. The formulation of a geometrically exact beam can be described by the position vector of the beam centerline with a rotation matrix of the rotation of a cross-section. The curvature vector is used to describe the rotational strain (bending and torsion) of the beam. The shear-locking problem for slender beam due to the independent interpolations of displacement and rotation can be avoided by the modification of the formulation of the geometrically exact beam element. Shabana (Shabana and Yakoub, 2001) and Yakouba (Yakoub and Shabana, 2001) developed a formulation called absolute nodal coordinate for the beam element by selection 12 degrees of freedom for each node including position vectors and nine slopes. The shape function they designed can represent arbitrary large rigid body motions exactly. Zupan proposed a beam element formulation based on the interpolation of the curvatures, a strain measure-interpolation based element (Zupan and Saje, 2003). Zhang (Zhang et al., 2015) presented a coupled interpolation of the centerline position vector and the orientation vector of the cross-section to avoid the "shear lock" problem. Fang (Fang and Qi, 2016) a hybrid interpolation method, using Hermitian interpolation of the centerline to calculate the curvatures of the two end nodes and a second interpolation for the internal curvatures.

In this paper, the long boom manipulator with a folding boom system is investigated. The boom structure is modeled as a flexible spatial beam, meanwhile, the hydraulic cylinder and the luffing links are treated as rigid bodies. The governing equations of the entire manipulator are formulated according to the multi-body formulation with constrains. The flexible body is considered as geometrically exact Euler-Bernoulli beam, and a hybrid interpolation is proposed. Each beam is meshed by nodes that have the given global position vectors. And the derivatives of the curvatures of the beam centerline at these inner nodes are deter-

mined by the values of the two end nodes according to the cubic spline interpolation. The virtual power of each element can be formulated by the Gauss integration using the selected Gauss points. The parameters at these Gauss points between the two adjacent nodes can be described as the polynomials of the node parameters. Then the governing equations of the manipulator can be derived from the sum virtual power of the flexible beams and the rigid bodies.

2 MULTI-BODY DYNAMIC OF LONG BOOM MANIPULATOR

As shown in Fig. (1), the folding boom manipulator consists of two boom structure with the corresponding luffing mechanism. The luffing mechanism for the first boom (attached on the turntable) is a single hydraulic cylinder and the one for the second boom a hydraulic cylinder combining with two rigid links. The luffing operation means to change the angle between the boom and the horizontal level. The slew operation is the rotation motion of the turntable around the rotation axis. For simplicity, the original boom structure is modeled as a homogeneous flexible beam, and the hydraulic cylinders and the links are modeled as rigid bodies.
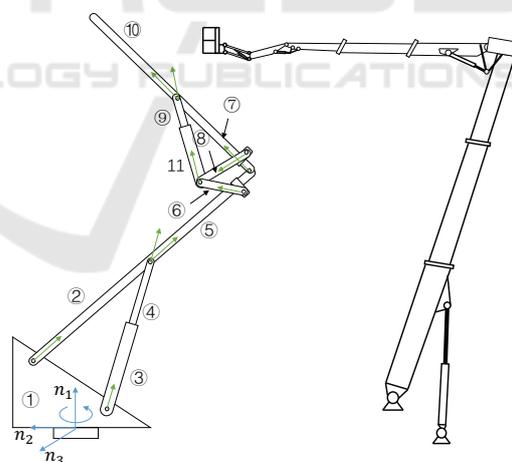

Figure 1: A folding boom system.

2.1 Multi-body Dynamics Formulation with Constraints

As marked in Fig. (1), body 2,5,7 and 10 are considered as flexible bodies, and body 1,3,4,6,8,9 and 11 are considered as rigid bodies. The body-fixed frames for the bars are defined as: 1) the origin is set at one end of the bar with rotational joint; 2) the first frame

vector is set along the bar at inertial time; 3) the third frame vector is set vertical to the luffing plane.

The origin of the body-fixed frame can be defined as

$$\boldsymbol{r}_{j,0} = \boldsymbol{r}_{k,0} + x_j \boldsymbol{n}_k^1 + y_j \boldsymbol{n}_k^2 \qquad (1)$$

where (x_j, y_j) is the origin coordinate of frame j in frame k.

For each rigid body, its moment of inertia relative to its own frame is $J_{j,c}$, and its mass center can be expressed as

$$\boldsymbol{r}_{j,c} = \boldsymbol{r}_{j,0} + u_j \boldsymbol{n}_j^1 + v_j \boldsymbol{n}_j^2 \qquad (2)$$

where (u_j, v_j) is the coordinate of the mass center in frame j.

The virtual power equation of each body can be expressed as

$$\delta p_j = \delta \begin{bmatrix} \dot{\boldsymbol{r}}_{j,0} \\ \boldsymbol{\omega}_j \end{bmatrix}^{\mathrm{T}} \left(\boldsymbol{M}_j \begin{bmatrix} \ddot{\boldsymbol{r}}_{j,0} \\ \dot{\boldsymbol{\omega}}_j \end{bmatrix} + \boldsymbol{F}_j \right) \qquad (3)$$

The relationship between virtual velocity and generalized virtual velocity is

$$\delta \begin{bmatrix} \dot{\boldsymbol{r}}_{j,0} \\ \boldsymbol{\omega}_j \end{bmatrix}^{\mathrm{T}} = \boldsymbol{T}_j \delta \dot{\boldsymbol{q}}, \begin{bmatrix} \ddot{\boldsymbol{r}}_{j,0} \\ \dot{\boldsymbol{\omega}}_j \end{bmatrix} = \boldsymbol{T}_j \ddot{\boldsymbol{q}} + \boldsymbol{\alpha}_j \qquad (4)$$

where $\boldsymbol{T}_j$ is the transfer matrix and $\boldsymbol{\alpha}_j = \dot{\boldsymbol{T}}_j \dot{\boldsymbol{q}}$.

Then the virtual power equation of all the bodies in the generalized coordinate can be expressed as

$$\delta p = \delta \dot{\boldsymbol{q}}^{\mathrm{T}} (\boldsymbol{M}\ddot{\boldsymbol{q}} + \boldsymbol{F}) \qquad (5)$$

where $\boldsymbol{M} = \sum \boldsymbol{T}_j^{\mathrm{T}} \boldsymbol{M}_j \boldsymbol{T}_j, \boldsymbol{F} = \sum \boldsymbol{T}_j^{\mathrm{T}} \boldsymbol{F}_j \boldsymbol{T}_j$

The virtual equation of hydraulic cylinder can be simplified as

$$\delta p_f = \delta \dot{s}(ks + c\dot{s}) \qquad (6)$$

where k is the equivalent stiffness, c is the equivalent dumping coefficient and s is the distant between the two joints on the cylinder.

The bodies of the system are connected by rotational or transnational joints. These kinematic constraints can be described as

$$\boldsymbol{\Phi}(\boldsymbol{q},t) = 0, \dot{\boldsymbol{\Phi}} = \boldsymbol{\Phi}_q \dot{\boldsymbol{q}} + \boldsymbol{\upsilon} = 0, \ddot{\boldsymbol{\Phi}} = \boldsymbol{\Phi}_q \ddot{\boldsymbol{q}} + \boldsymbol{\gamma} = 0 \ (7)$$

where $\boldsymbol{\upsilon} = \partial \boldsymbol{\Phi}/\partial t$, $\boldsymbol{\gamma} = \dot{\boldsymbol{\Phi}}_q \dot{\boldsymbol{q}} + \dot{\boldsymbol{\upsilon}}$ and $\boldsymbol{\Phi}_q$ is the Jacobian matrix of the constraints.

By using the stabilization of constraints proposed by Baumgerte(Baumgarte, 1972), the constraint equation of the acceleration can be rewritten as

$$\boldsymbol{\Phi}_q \ddot{\boldsymbol{q}} + \dot{\boldsymbol{\Phi}}_q \dot{\boldsymbol{q}} + \dot{\boldsymbol{\Phi}}_t + 2\xi_1 \dot{\boldsymbol{\Phi}} + \xi_2 \boldsymbol{\Phi} = 0 \qquad (8)$$

where ξ_1 and ξ_2 are the stabilization coefficients.

2.2 Geometrically Exact Euler-Bernoulli Beam

2.2.1 The Geometric Configuration of a Spatial Beam

The main assumption of a 3D Euler-Bernoulli beam theory is that arbitrary cross sections of the beam always maintain rigid and perpendicular to the tangent vector of the central line of the beam. The position vector $\boldsymbol{r}(s)$ of the beam central line is defined with the arc-length coordinate of the beam central line s.
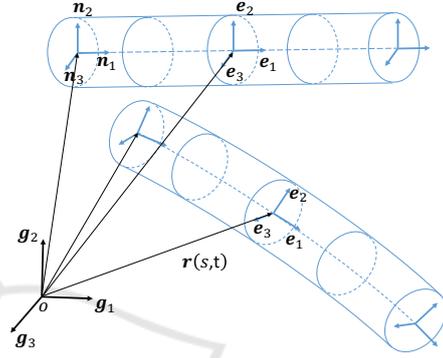

Figure 2: Geometic configuration of a Euler-Bernulli beam.

The basis frame of the cross section is define as $[\boldsymbol{e}_1, \boldsymbol{e}_2, \boldsymbol{e}_3]$, in which $\boldsymbol{e}_1$ is parallel to the tangent vector of the beam central line $\boldsymbol{r}'$.

$$\boldsymbol{e}_1 = \boldsymbol{r}' / \|\boldsymbol{r}'\| \qquad (9)$$

And the other two orientaiton vectors are atteched on the cross section and denoted by the right-handed orthogonal rule.

$$\boldsymbol{e}_2^{\mathrm{T}} \boldsymbol{r}' = \boldsymbol{e}_3^{\mathrm{T}} \boldsymbol{r}' = 0 \qquad (10)$$

The normal vector of the cross section can be expressed as ($s_i = \sin\varphi_i, c_i = \cos\varphi_i$)

$$\boldsymbol{e}_1 = c_2 c_3 \boldsymbol{n}_1 + s_3 \boldsymbol{n}_2 - s_2 c_3 \boldsymbol{n}_3 \qquad (11)$$

and the Euler angles can be calculated as

$$\begin{aligned} \varphi_2 &= \mathrm{acrtan}(-\boldsymbol{n}_3^{\mathrm{T}} \boldsymbol{e}_1 / \boldsymbol{n}_1^{\mathrm{T}} \boldsymbol{e}_1) \\ \varphi_3 &= \mathrm{acrsin}(\boldsymbol{n}_2^{\mathrm{T}} \boldsymbol{e}_1) \end{aligned} \qquad (12)$$

The rotation matrix of the coordinate system of the cross section with respect ot the basis frame of the beam can described by Euler angles as

$$\boldsymbol{e}_i = \boldsymbol{R}\boldsymbol{n}_i = \begin{bmatrix} \boldsymbol{e}_1 & \boldsymbol{e}_2 & \boldsymbol{e}_3 \end{bmatrix} \boldsymbol{n}_i \qquad (13)$$

2.2.2 The Formulation of Angle Velocity of the Cross-section

The time derivative of the base vectors of the reference frame on the cross section can be obtained by the cross product of its angle velocity and the base vectors

$$\dot{\mathbf{e}}_i = \widetilde{\boldsymbol{\omega}}\mathbf{e}_i = \boldsymbol{\omega} \times \mathbf{e}_i \qquad (14)$$

The angle velocity vector of the cross section can be expressed as

$$\boldsymbol{\omega} = \omega_{e1}\boldsymbol{e}_1 + \omega_{e2}\boldsymbol{e}_2 + \omega_{e3}\boldsymbol{e}_3 \qquad (15)$$

in which the weight value can be calculated as

$$\omega_{e1} = \boldsymbol{e}_3^{\mathrm{T}}\dot{\boldsymbol{e}}_2, \omega_{e2} = \boldsymbol{e}_1^{\mathrm{T}}\dot{\boldsymbol{e}}_3, \omega_{e3} = \boldsymbol{e}_2^{\mathrm{T}}\dot{\boldsymbol{e}}_1 \qquad (16)$$

Then the formulation of the angle velocity of cross section can be written as

$$\boldsymbol{\omega} = \boldsymbol{T}_{\varphi}\dot{\boldsymbol{\varphi}} \qquad (17)$$

where

$$\boldsymbol{T}_{\varphi} = \begin{bmatrix} 1 & s_3 & 0 \\ 0 & c_1c_3 & -s_1 \\ 0 & -s_1c_3 & -c_1 \end{bmatrix} = \begin{bmatrix} \boldsymbol{p}_1 & \boldsymbol{p}_2 & \boldsymbol{p}_3 \end{bmatrix}$$

$\boldsymbol{p}_1, \boldsymbol{p}_2$ and $\boldsymbol{p}_3$ are the weight vectors of three rotation axis in the frame of the cross section.

The angler accelerations of the cross section can be expressed as

$$\dot{\boldsymbol{\omega}} = \boldsymbol{T}_{\varphi}\ddot{\boldsymbol{\varphi}} + \dot{\boldsymbol{T}}_{\varphi}\dot{\boldsymbol{\varphi}} \qquad (18)$$

2.2.3 The Formulation of Strain Vector of the Cross-section

The curvature vector of the cross section represents the bending and torsion of the centerline of the beam. And the arc-length derivative of the base vectors of the reference frame on the cross section can be obtained by the cross product of the curvature vector and the base vectors

$$\boldsymbol{e}_i' = \widetilde{\boldsymbol{\kappa}}\mathbf{e}_i = \boldsymbol{\kappa} \times \mathbf{e}_i \qquad (19)$$

The curvature vector on the cross section can be expressed as

$$\boldsymbol{\kappa} = \kappa_{e1}\boldsymbol{e}_1 + \kappa_{e2}\boldsymbol{e}_2 + \kappa_{e3}\boldsymbol{e}_3 \qquad (20)$$

$$\kappa_{e1} = \boldsymbol{e}_3^{\mathrm{T}}\boldsymbol{e}_2', \kappa_{e2} = \boldsymbol{e}_1^{\mathrm{T}}\boldsymbol{e}_3', \kappa_{e3} = \boldsymbol{e}_2^{\mathrm{T}}\boldsymbol{e}_1' \qquad (21)$$

$$\boldsymbol{\kappa} = \boldsymbol{T}_{\varphi}\boldsymbol{\varphi}' \qquad (22)$$

The time derivatives of $\boldsymbol{\kappa}$ and $\boldsymbol{\kappa}'$ are

$$\dot{\boldsymbol{\kappa}} = \boldsymbol{T}_{\varphi}\dot{\boldsymbol{\varphi}}' + \boldsymbol{\phi}(\boldsymbol{\varphi}')\dot{\boldsymbol{\varphi}} \qquad (23)$$

where

$$\boldsymbol{\phi}(\boldsymbol{\varphi}') = \begin{bmatrix} \frac{\partial \boldsymbol{p}_2}{\partial \varphi_1}\varphi_2' + \frac{\partial \boldsymbol{p}_3}{\partial \varphi_1}\varphi_3' & \mathbf{0} & \frac{\partial \boldsymbol{p}_2}{\partial \varphi_3}\varphi_2' \end{bmatrix}$$

According to the geometrically exact beam theory, the generalized strains can be classified as axial strain and the three weights of curvature vector in the frame of cross-section.

$$\varepsilon_1 = \|\boldsymbol{r}'\| - 1 \qquad (24)$$

and its time derivatives can be expressed as

$$\dot{\varepsilon}_1 = \boldsymbol{T}_{\varepsilon}\dot{\boldsymbol{r}}' \qquad (25)$$

in which

$$\boldsymbol{T}_{\varepsilon} = (1 + \varepsilon_1)^{-1}(\boldsymbol{r}')^{\mathrm{T}}$$

The derivative of the normal vector with the respect of the arc-length is

$$\boldsymbol{e}_1' = (1 + \varphi_1)^{-1}(\boldsymbol{r}'' - \varepsilon_1'\boldsymbol{e}_1) = \boldsymbol{b}_2\varphi_2' + \boldsymbol{b}_3\varphi_3' \qquad (26)$$

in which

$$\boldsymbol{b}_2 = -s_2c_3\boldsymbol{n}_1 - c_2c_3\boldsymbol{n}_3$$
$$\boldsymbol{b}_3 = -c_2s_3\boldsymbol{n}_1 + c_3\boldsymbol{n}_2 + s_2s_3\boldsymbol{n}_3$$

Then the arc-length derivatives of Euler angles can be acquired as

$$\varphi_2' = \boldsymbol{b}_2^{\mathrm{T}}\boldsymbol{e}_1, \varphi_3' = \boldsymbol{b}_3^{\mathrm{T}}\boldsymbol{e}_1 \qquad (27)$$

The time derivative of normal vector can be expressed as

$$\dot{\boldsymbol{e}}_1 = (1 + \varepsilon_1)^{-1}(\boldsymbol{E} - \boldsymbol{e}_1\boldsymbol{e}_1^{\mathrm{T}})\dot{\boldsymbol{r}}' = \boldsymbol{b}_2\dot{\varphi}_2 + \boldsymbol{b}_3\dot{\varphi}_3 \qquad (28)$$

then the time derivative of Euler angles can be expressed as

$$\dot{\varphi}_2 = \boldsymbol{b}_2^{\mathrm{T}}\dot{\boldsymbol{e}}_1 = \boldsymbol{T}_{\varphi_2}\dot{\boldsymbol{r}}', \dot{\varphi}_3 = \boldsymbol{b}_3^{\mathrm{T}}\dot{\boldsymbol{e}}_1 = \boldsymbol{T}_{\varphi_3}\dot{\boldsymbol{r}}' \qquad (29)$$

where the transfer matrices are

$$\boldsymbol{T}_{\varphi_2} = \boldsymbol{b}_2^{\mathrm{T}}(1 + \varepsilon_1)^{-1}(\boldsymbol{E} - \boldsymbol{e}_1\boldsymbol{e}_1^{\mathrm{T}})$$
$$\boldsymbol{T}_{\varphi_3} = \boldsymbol{b}_3^{\mathrm{T}}(1 + \varepsilon_1)^{-1}(\boldsymbol{E} - \boldsymbol{e}_1\boldsymbol{e}_1^{\mathrm{T}})$$

The further arc-length derivative can be expressed as

$$\dot{\varphi}_2' = \boldsymbol{T}_{\varphi_2}\dot{\boldsymbol{r}}'' + \boldsymbol{T}_{\varphi_2}'\dot{\boldsymbol{r}}', \dot{\varphi}_3' = \boldsymbol{T}_{\varphi_3}\dot{\boldsymbol{r}}'' + \boldsymbol{T}_{\varphi_3}'\dot{\boldsymbol{r}}' \qquad (30)$$

where

$$\boldsymbol{T}_{\varphi_2}' = (1 + \varepsilon_1)^{-1}(\boldsymbol{b}_2'^{\mathrm{T}} - \varepsilon_1'\boldsymbol{T}_{\varphi_2})$$
$$\boldsymbol{T}_{\varphi_3}' = (1 + \varepsilon_1)^{-1}(\boldsymbol{b}_3'^{\mathrm{T}} - \varepsilon_1'\boldsymbol{T}_{\varphi_3})$$

2.2.4 Discretization Method

The main idea of the discretization is to add $n-1$ nodes on the beam centerline and to mesh the whole beam into n elements. In order to reduce the number of system variables, the position vectors $\boldsymbol{r}_i$ of all nodes and the arc-length derivatives of the position vectors $\boldsymbol{r}'_0, \boldsymbol{r}'_n$ of two boundary nodes are selected. And the arc-length derivatives of position vectors of the inner nodes $(\boldsymbol{r}'_i, i = 1, 2, ..., n-1)$ can be acquired by the following equations with cubic spline interpolation

$$[\boldsymbol{r}']\boldsymbol{A} = a[\boldsymbol{r}]\boldsymbol{B} + [\ \boldsymbol{r}'_0 \quad \boldsymbol{r}'_n\ ]\boldsymbol{C} \tag{31}$$

where $a = L_{-1}$, $[\boldsymbol{r}'] = [\ \boldsymbol{r}'_0 \quad \boldsymbol{r}'_1 \quad ... \quad \boldsymbol{r}'_n\ ]$ and $[\boldsymbol{r}] = [\ \boldsymbol{r}_0 \quad \boldsymbol{r}_1 \quad ... \quad \boldsymbol{r}_n\ ]$

Then time derivations of the curvature of the inner nodes can be expressed by the parameters of the boundary nodes as

$$\dot{\boldsymbol{r}}'_i = \boldsymbol{\Gamma}_i \dot{\boldsymbol{q}}_e \tag{32}$$

and

$$\ddot{\boldsymbol{r}}'_i = \boldsymbol{\Gamma}_i \ddot{\boldsymbol{q}}_e + \boldsymbol{\gamma}_i \tag{33}$$

where $\boldsymbol{\gamma}_i$ is the acceleration margin and the details are not expanded.

The arc-length coordinate of the node i on the centroid line of the beam can be given as

$$s_i = i L_0 / n \tag{34}$$

in which L_0 is the original length of the beam and n is the number of the elements meshed on the beam.

The position vector of the point between each two nodes on the centerline of the beam can be described by the polynomials as

$$\boldsymbol{r}^\xi = N_1 \boldsymbol{r}_i + L N_2 \boldsymbol{r}'_i + N_3 \boldsymbol{r}_{i+1} + L N_4 \boldsymbol{r}'_{i+1} \tag{35}$$

where $L = L_0 / n$ and the shape functions are

$$N_1 = 1 - 3\xi^2 + 2\xi^3, N_2 = \left(\xi - 2\xi^2 + \xi^3\right)$$
$$N_3 = 3\xi^2 - 2\xi^3, N_4 = \left(\xi^3 - \xi^2\right) \tag{36}$$

And the normalized variables are defined as

$$\xi = L^{-1}(s - s_1) \tag{37}$$

Furthermore, the curvature on the centerline of the beam between two nodes and its arc-length derivation can be expressed with the derivations of the shape functions. The overall idea of the hybrid interpolation of an entire Euler-Bernoulli beam is show as Fig. (3). Then the time derivative of the position vector at the point between each nodes can be expressed as

$$\dot{\boldsymbol{r}}^\xi = \boldsymbol{T}_r \dot{\boldsymbol{q}}_e, \ddot{\boldsymbol{r}}^\xi = \boldsymbol{T}_r \ddot{\boldsymbol{q}}_e + \boldsymbol{a}_r \tag{38}$$

in which

$$\boldsymbol{T}_r = N_1 \boldsymbol{G}_i + N_3 \boldsymbol{G}_{i+1} + L(N_2 \boldsymbol{\Gamma}_i + N_4 \boldsymbol{\Gamma}_{i+1})$$
$$\boldsymbol{a}_r = L(N_2 \boldsymbol{\Gamma}_i + N_4 \boldsymbol{\Gamma}_{i+1})$$
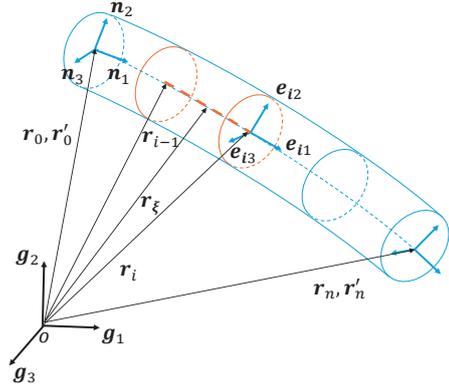

Figure 3: Hybrid interpolation of an Euler-Bernoulli beam.

2.2.5 The Virtual Power of the Beam Element

The virtual power of the entire beam is formed by the sum of virtual power from each element.

The virtual power of inertial forces

$$\delta p_{\text{tra}} = m \int_0^1 \delta \dot{\boldsymbol{r}}^{\xi \text{T}} (\ddot{\boldsymbol{r}}^\xi - \boldsymbol{g}) d\xi$$
$$= \delta \dot{\boldsymbol{q}}_e^{\text{T}} (\boldsymbol{M}_{\text{e,tra}} \ddot{\boldsymbol{q}}_e + \boldsymbol{F}_{\text{e,tra}}) \tag{39}$$

where

$$\boldsymbol{M}_{\text{e,tra}} = mL \int_0^1 \boldsymbol{T}_r^{\text{T}} \boldsymbol{T}_r d\xi$$

$$\boldsymbol{F}_{\text{e,tra}} = mL \int_0^1 \boldsymbol{T}_r^{\text{T}} (\boldsymbol{a}_r - \boldsymbol{g}) d\xi$$

The virtual kinetic power of rotation can be expressed as

$$\delta p_{\text{rot}} = L \int_0^1 \delta \boldsymbol{\omega}^{\text{T}} \left(\boldsymbol{J}_\rho \dot{\boldsymbol{\omega}} + \widetilde{\boldsymbol{\omega}} \boldsymbol{J}_\rho \boldsymbol{\omega}\right) d\xi$$
$$= \delta \dot{\boldsymbol{q}}_e^{\text{T}} (\boldsymbol{M}_{\text{e,rot}} \ddot{\boldsymbol{q}}_e + \boldsymbol{F}_{\text{e,rot}}) \tag{40}$$

where

$$\boldsymbol{M}_{\text{e,rot}} = L \int_0^1 \boldsymbol{T}_\varphi^{\text{T}} \boldsymbol{R}^{\text{T}} \boldsymbol{J}_\rho \boldsymbol{R} \boldsymbol{T}_\varphi d\xi$$

$$\boldsymbol{F}_{\text{e,rot}} = L \int_0^1 \boldsymbol{T}_\varphi^{\text{T}} \left(\boldsymbol{R}^{\text{T}} \boldsymbol{J}_\rho \boldsymbol{R} \dot{\boldsymbol{T}}_\varphi \dot{\boldsymbol{q}}_e + \widetilde{\boldsymbol{\omega}} \boldsymbol{J}_\rho \boldsymbol{\omega}\right) d\xi$$

The strain vector is

$$\boldsymbol{\varepsilon} = \left[\ \varepsilon_1 \quad \kappa_1 \quad \kappa_2 \quad \kappa_3\ \right]^{\text{T}} \tag{41}$$

The internal virtual power can be express as

$$\delta p_{\text{int}} = L \int_0^1 \delta \dot{\boldsymbol{\varepsilon}}^{\text{T}} \boldsymbol{D} \boldsymbol{\varepsilon} d\xi = (\delta \dot{\boldsymbol{q}}_e)^{\text{T}} \boldsymbol{F}_{\text{e,int}}(\boldsymbol{q}_e) \tag{42}$$

where $\boldsymbol{D} = \text{diag}(EA, GJ, EI_2, EI_3)$ and $\boldsymbol{F}_{\text{e,int}}(\boldsymbol{q}_e)$ is called generalized nodal forces

$$\boldsymbol{F}_{\text{e,int}}(\boldsymbol{q}_e) = L \int_0^1 (\frac{\partial \boldsymbol{\varepsilon}}{\partial \boldsymbol{q}_e})^{\text{T}} \boldsymbol{D} \boldsymbol{\varepsilon} d\xi \tag{43}$$

The external virtual power can be written as

$$\delta p_{\text{ext}} = \delta \dot{\boldsymbol{r}}_i^{\text{T}} \boldsymbol{f}_i + \delta \boldsymbol{\omega}_i^{\text{T}} \boldsymbol{m}_i + \int_0^1 \delta \dot{\boldsymbol{r}}^{\xi \text{T}} \boldsymbol{f}(\xi) d\xi \quad (44)$$

where $\boldsymbol{f}_i$ and $\boldsymbol{m}_i$ are the concentrated forces and moments on the element node i and $\boldsymbol{f}(\xi)$ is the distributed force. The virtual work of the external forces can be reformed as

$$\delta p_{\text{ext}} = \delta \dot{\boldsymbol{q}}_e^{\text{T}} (\boldsymbol{F}_{\text{c}} + \boldsymbol{F}_{\text{d}}) = \delta \dot{\boldsymbol{q}}_e^{\text{T}} \boldsymbol{F}_{\text{e,ext}} \quad (45)$$

where the generalized external forces are

$$\boldsymbol{F}_{\text{c}} = \boldsymbol{F}_i + \boldsymbol{R}^{\text{T}} \boldsymbol{T}_\varphi^{\text{T}} \boldsymbol{M}_i, \boldsymbol{F}_{\text{d}} = \int_0^1 \boldsymbol{T}_r \boldsymbol{f}(\xi) d\xi$$

2.3 The Governing Dynamic Equation

According to the virtual power principle, the virtual power equation of a single beam element is

$$\delta p_{\text{int}} + \delta p_{\text{ine}} = \delta p_{\text{ext}} \quad (46)$$

By submitting the internal virtual power, inertial virtual power and the external virtual power, the equation yields as

$$\delta \boldsymbol{q}_e^{\text{T}} (\boldsymbol{M}_{\text{e,ine}} \ddot{\boldsymbol{q}}_e + \boldsymbol{F}_{\text{e,ine}} + \boldsymbol{F}_{\text{e,int}} - \boldsymbol{F}_{\text{e,ext}}) = 0 \quad (47)$$

the the governing dynamic equation of beam element can be expressed as

$$\boldsymbol{M}_e \ddot{\boldsymbol{q}}_e + \boldsymbol{F}_e = 0 \quad (48)$$

where $\boldsymbol{F}_e = \boldsymbol{F}_{\text{e,ine}} + \boldsymbol{F}_{\text{e,int}} - \boldsymbol{F}_{\text{e,ext}}$.

The general coordinate is defined as $\boldsymbol{q}$, and the the coordinate of the nodes in the element form can be written as

$$\boldsymbol{q}_{e,i} = \boldsymbol{T}_i \boldsymbol{q}, \dot{\boldsymbol{q}}_{e,i} = \boldsymbol{T}_i \dot{\boldsymbol{q}}, \ddot{\boldsymbol{q}}_{e,i} = \boldsymbol{T}_i \ddot{\boldsymbol{q}} + \dot{\boldsymbol{T}}_i \dot{\boldsymbol{q}} \quad (49)$$

The original dynamic equation of multi-body system can be expanded to a dynamic equation of flexible-rigid multi-body system with constraints by using Lagrange multiplier as

$$\boldsymbol{M} \ddot{\boldsymbol{q}} - \boldsymbol{F} = \boldsymbol{\Phi}_q^{\text{T}} \lambda \quad (50)$$

where

$$\boldsymbol{M} = \sum \boldsymbol{T}_i^{\text{T}} \boldsymbol{M}_{e,i} \boldsymbol{T}_i + \sum \boldsymbol{T}_j^{\text{T}} \boldsymbol{M}_j \boldsymbol{T}_j,$$
$$\boldsymbol{F} = \sum \boldsymbol{T}_i^{\text{T}} (\boldsymbol{M}_{e,i} \dot{\boldsymbol{T}}_i \dot{\boldsymbol{q}} + \boldsymbol{F}_{e,i}) + \sum \boldsymbol{T}_j^{\text{T}} \boldsymbol{F}_j \boldsymbol{T}_j$$

Then, the governing equation can be rewritten as

$$\begin{bmatrix} \boldsymbol{M} & \boldsymbol{\Phi}_q^{\text{T}} \\ \boldsymbol{\Phi}_q & 0 \end{bmatrix} \begin{bmatrix} \ddot{\boldsymbol{q}} \\ -\lambda \end{bmatrix} = \begin{bmatrix} \boldsymbol{F} \\ -\dot{\boldsymbol{\Phi}}_q \dot{\boldsymbol{q}} - \dot{\boldsymbol{\Phi}}_t - 2\xi_1 \dot{\boldsymbol{\Phi}} - \xi_2 \boldsymbol{\Phi} \end{bmatrix} \quad (51)$$

which can be transferred into the order ordinary differential equations (ODEs) about q and can be solved by ODE solvers.

3 SIMULATION AND ANALYSIS

3.1 Initial Configuration and Parameters

The linear motions of two hydraulic cylinders and rotational motion of the turntable are designed as following functions of velocity and acceleration, which are given as

$$v(t) = \begin{cases} v_0 t^2 (3t_1 - 2t) / t_1^3 & 0 < t < t_{\text{a}} \\ v_0 & t_{\text{a}} < t < t_{\text{b}} \\ v_0 (t_1 + t_2 + t_3 - t) / t_3 & t_{\text{b}} < t < t_{\text{c}} \end{cases}$$
$$a(t) = \begin{cases} 6v_0 t (t_1 - t) / t_1^3 & 0 < t < t_{\text{a}} \\ 0 & t_{\text{a}} < t < t_{\text{b}} \\ -v_0 / t_3 & t_{\text{b}} < t < t_{\text{c}} \end{cases} \quad (52)$$

where $t_{\text{a}} = t_1$, $t_{\text{b}} = t_1 + t_2$ and $t_{\text{c}} = t_1 + t_2 + t_3$.

The parameters of the rigid bodies, such as the hydraulic cylinders and the rigid links are chosen as follows: the masses of the cylinders and the pistons are both 10kg, the radiuses of the cross-section of the cylinders and the pistons are 0.05m and 0.035m, the linear density and the radius of the links are 61.5kg/m and 0.05m. And the parameters of the flexible bodies are selected as: the radius of the cross-section is 0.15m; the linear density is 544.6kg/m; the elastic modulus is 2.11×10^{11}Pa and the Poisson's ratio is 0.3.

The initial configuration of the manipulator is designed as Fig. (4). Both hydraulic cylinders are retracted, the first boom is at horizontal position and the second boom is folded and coinciding with the first boom. The luffing plane is set in XY-plane.
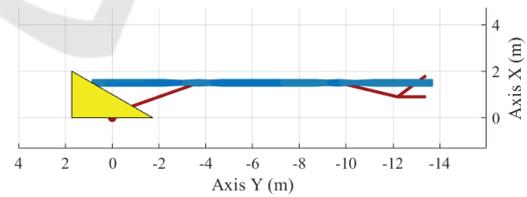

Figure 4: The initial configuration of the manipulator.

The Fig. (5) presents the deployment sequence of the manipulator in the designed scenario. First, the first boom is driven to luff, when the first hydraulic cylinder is fully extended, the first boom arrives at the designed angle displacement (stage 1). Then the turntable rotates clockwise 90° and changes the luffing plane from X-Y plane to X-Z plane (stage 2). At last, the second boom starts and the first boom remains static and the tip of the second boom reaches the highest position at last (stage 3).
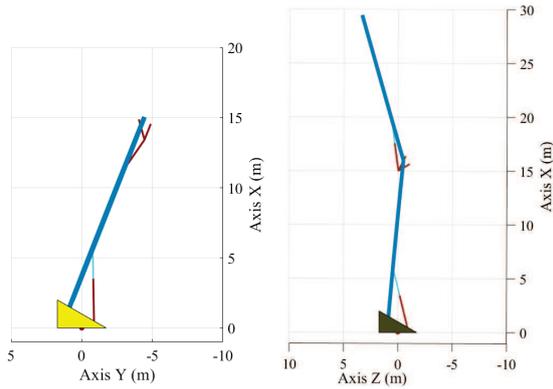
Figure 5: Four configurations of the manipulator during the operation.

3.2 Simulation Results and Analysis

The dynamic equations of the flexible multi-body system are usually stiff differential equations. Different from the common numerical method to solve stiff equations using numerical damping to filter the high frequency, we apply the method presented by Qi (Qi et al., 2018) to filter the high-frequency part during the modeling stage. The main idea of this method is to use the average value of the stress $\bar{\sigma}$ in the time interval $(t, t+h)$ to approximate the instantaneous stress σ as

$$\bar{\sigma} \triangleq h^{-1} \int_t^{t+h} \sigma_\tau \mathrm{d}\tau \approx \sigma_t + h\dot{\sigma}_t/2 + h^2\ddot{\sigma}_t/6 \quad (53)$$

then, the filtered equation can be solved by regular ODE solver in MATLAB, such as solver ODE45.

The motion designed in section 3.1 is simulated and solved with ODE45 in MATLAB. The coefficient is selected as 0.005. The curves in Fig. (6) show the displacements of the tip of the second boon in the coordinate space.
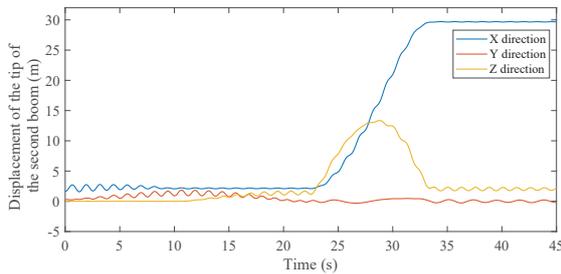

Figure 6: The displacement of the boom's tip.

The Fig.(7) and Fig.(8) represent the results with different selection of the value of h. The solid line is the results solved by ode45 with $h = 0.001$ and $h = 0.002$ which means the frequencies higher than 1000Hz and 500Hz have been filtered. The dotted

line is the results solved by stiff solver ode15s. In this caparison, we simulated the luffing process only.
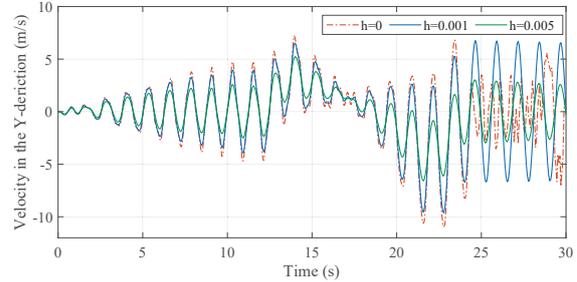

Figure 7: The velocity of the tip of the second boom in the Y direction.
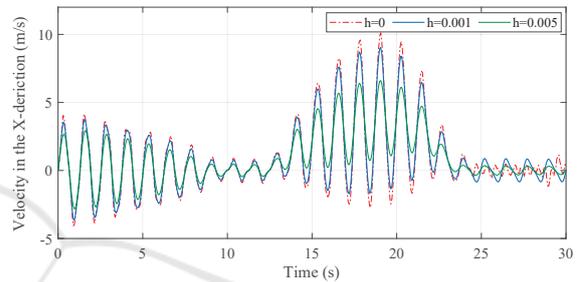

Figure 8: The velocity of the tip of the second boom in the X direction.

The above figures show that some high frequencies parts of the stiff system have been filtered, especially at the rare part of the simulation when no more input motion occurs. The amplitude of the dynamic response is also reduced as long as the coefficient h increases.

4 CONCLUSION AND OUTLOOK

In this paper, we introduce the basic theory of the geometrically exact Euler-Bernoulli beam and apply a hybrid interpolation method to discrete the beam. The cubic spline interpolation is used to reduce the number of the system variables by describing the arc-length derivatives of the inner nodes with the position vectors of all the nodes and the arc-length derivatives of the two boundary nodes. The virtual power of the element is formulated by the Gauss integration between each adjective two nodes. The system parameters inside the element are presented as the interpolation using the Gauss points between the two nodes of the element. Then the governing equations of the flexible bodies can be derived, and combining the governing equations of the rigid bodies and constrains function, the dynamic governing equations of the folding boom system are formulated with a method of fil-

tering high frequency vibrations and solved by ODE solver. The dynamic simulation of the designed long boom manipulator in a process with luffing and slewing motions is accomplished.

The following topics are considered as our further research with the object to control the vibration of the long boom manipulator in the operation:

1).In the current model, the elasticity of the hydraulic cylinder is simplified as constant spring stiffness. In reality, the oil inside the chambers of the hydraulic cylinder performs as a nonlinear elastic body. The equations describing the dynamics of the hydraulic system will be included in the model of the long boom manipulator to acquire a more accurate dynamic response of the system.

2). Although the motions of the manipulator are designed to be smooth, the dynamic response of the boom system is still remarkable due to the large flexibility of the structure. The mathematical description of the system will be reformed as an optimal control problem to investigate the solution of vibration control. The optimal control problem can be proposed as a path-following problem to optimize the dynamic response of the boom structure to fit the trajectory of the motion of the model with a rigid body assumption.

ACKNOWLEDGEMENTS

REFERENCES

Baumgarte, J. (1972). Stabilization of constraints and integrals of motion in dynamical systems. *Computer methods in applied mechanics and engineering*, 1(1):1–16.

Fang, H. and Qi, Z. (2016). A hybrid interpolation method for geometric nonlinear spatial beam elements with explicit nodal force. *Mathematical Problems in Engineering*, 2016.

Gao, L., Wang, M., Kleeberger, M., Peng, H., and Fottner, J. (2019). Modeling and discretization of hydraulic actuated telescopic boom system in port-hamiltonian formulation. *Modeling and Discretization of Hydraulic Actuated Telescopic Boom System in Port-Hamiltonian Formulation. In Proceedings of the 9th International Conference on Simulation and Modeling Methodologies, Technologies and Applications*, (69-79):SCITEPRESS–Science and Technology Publications, Lda.

Nguyen, V. T., Schmidt, T., and Leonhardt, T. (2019). Effect of pre-tensioned loads to vibration at the ladder

tip in raising and lowering processes on a turntable ladder. *Journal of Mechanical Science and Technology*, 33(5):2003–2010.

Pertsch, A. and Sawodny, O. (2016). Modelling and control of coupled bending and torsional vibrations of an articulated aerial ladder. *Mechatronics*, 33:34–48.

Pertsch, A., Zimmert, N., and Sawodny, O. (2009). Modeling a fire-rescue turntable ladder as piecewise euler-bernoulli beam with a tip mass. *In Proceedings of the 48h IEEE Conference on Decision and Control (CDC) held jointly with 2009 28th Chinese Control Conference*, (pp. 7321-7326).

Qi, Z., Cao, Y., and Wang, G. (2018). Model smoothing methods in numerical analysis of flexible multibody systems. *Chinese Journal of*, 50(4):863–870.

Reissner, E. (1972). On one-dimensional finite-strain beam theory: the plane problem. *Zeitschrift fuer angewandte Mathematik und Physik ZAMP*, 23(5):p 795–804.

Reissner, E. (1973). On one-dimensional large-displacement finitestrain beam theory. *Studies in AppliedMathematics*, 52(2):p 87–95.

Sawodny, O., Aschemann, H., and Bulach, A. (2002). Mechatronical designed control of fire-rescue turntable-ladders as flexible link robots. *IFAC Proceedings Volumes*(35):509–514.

Shabana, A. A. and Yakoub, R. Y. (2001). Three dimensional absolute nodal coordinate formulation for beam elements: theory. *J. Mech. Des.*, 123(4):606–613.

Simo, J. C. (1985). A finite strain beam formulation. the three-dimensional dynamic problem. i. *Computer methods in applied mechanics and engineering*, 49(1):55–70.

Simo, J. C. (1988). On the dynamics in space of rods undergoing large motions—a geometrically exact approach. *Computer methods in applied mechanics and engineering*, 66(2):125–161.

Simo, J. C. and Vu-Quoc, L. (1986). A three-dimensional finite-strain rod model. part ii: Computational aspects. *Computer methods in applied mechanics and engineering*, 58(1):79–116.

Yakoub, R. Y. and Shabana, A. A. (2001). Three dimensional absolute nodal coordinate formulation for beam elements: implementation and applications. *J. Mech. Des.*, 123(4):614–621.

Zhang, Z., Qi, Z., Wu, Z., and Fang, H. (2015). A spatial euler-bernoulli beam element for rigid-flexible coupling dynamic analysis of flexible structures. *Shock and Vibration*, 2015.

Zupan, D. and Saje, M. (2003). Finite-element formulation of geometrically exact three-dimensional beam theories based on interpolation of strain measures. *Computer methods in applied mechanics and engineering*, 192(49-50):5209–5248.

Zuyev, A. (2005). Stabilization of a flexible manipulator model with passive joints. *IFAC Proceedings Volumes*, 38(1):784–789.